Journal of Statistical Mechanics: Theory and Experiment
An IOP and SISSA journal

Interfacial depinning transitions in disordered media: revisiting an old puzzle

Belén Moglia[1,2], Ezequiel V Albano[1,2], Pablo Villegas[3] and Miguel A Muñoz[3]

[1] Instituto de Física de Líquidos y Sistemas Biológicos (IFLYSIB), Universidad Nacional de La Plata, CONICET CCT-La Plata, Calle 59 Nro 789, 1900 La Plata, Argentina
[2] Departamento de Física, Facultad de Ciencias Exactas, Universidad Nacional de La Plata, La Plata, Argentina
[3] Departamento de Electromagnetismo y Física de la Materia e Instituto Carlos I de Física Teórica y Computacional, Universidad de Granada, Facultad de Ciencias, E-18071, Granada, Spain
E-mail: mamunoz@onsager.ugr.es

Received 24 July 2014
Accepted for publication 3 September 2014
Published 15 October 2014

Online at stacks.iop.org/JSTAT/2014/P10024
doi:10.1088/1742-5468/2014/10/P10024

Abstract. Interfaces advancing through random media represent a number of different problems in physics, biology and other disciplines. Here, we study the pinning/depinning transition of the prototypical non-equilibrium interfacial model, i.e. the Kardar–Parisi–Zhang equation, advancing in a disordered medium. We will separately analyze the cases of positive and negative non-linearity coefficients, which are believed to exhibit qualitatively different behavior: the positive case shows a continuous transition that can be related to directed-percolation-depinning, while in the negative case there is a discontinuous transition and faceted interfaces appear. Some studies have argued from different perspectives that both cases share the same universal behavior. By using a number of computational and scaling techniques we will shed light on this puzzling situation and conclude that the two cases are intrinsically different.

Keywords: interfaces in random media (theory)

1742-5468/14/P10024+13$33.00

Contents

1. Introduction

The study and characterization of growing interfaces under non-equilibrium conditions is a topic of interdisciplinary interest [1–4]. Moving interfaces are often found in physics (crystal and amorphous material growth, polymers and colloids, granular matter, wetting, thin films), physical–chemistry (catalysis, corrosion, reaction front propagation), biology (cellular, fungal and bacterial colony growth, cell-sorting, wound healing, tumor expansion), etc. Understanding the properties of interfaces in relation to phenomena such as corrosion, adhesion, wetting, friction, micro- or nano-fluidics, etc is essential for the development of technological applications. Moreover, the study of interfaces is of fundamental interest as a typical problem in statistical mechanics as they constitute a canonical example of critical phenomena and generic scale-free behavior in systems away from thermal equilibrium.

Within this broad context, the Kardar–Parisi–Zhang (KPZ) dynamics [5] represents the simplest and broadest universality class of non-equilibrium growth [1–4]. Its study has been recently boosted by remarkable experimental and theoretical breakthroughs [6–14], which have triggered renewed interest. The KPZ interfacial dynamics is defined by the Langevin equation:

$$\partial_t h(\mathbf{x},t) = \nu\nabla^2 h(\mathbf{x},t) + \lambda(\nabla h(\mathbf{x},t))^2 + F + \eta(\mathbf{x},t), \tag{1}$$

where $h(\mathbf{x},t)$ is the local height of the interfaces, $F > 0$ is the driving force, $\eta(\mathbf{x},t)$ is the zero-mean delta-correlated Gaussian noise, the first term on the right-hand side (with

proportionality constant ν) describes the relaxation of the interface caused by the surface tension and finally $\lambda(\nabla h)^2$ is the dominant nonlinear term. This last term accounts for lateral growth and breaks the up–down symmetry in such a way that the interface is not invariant under the transformation $h \to -h$.

Interfacial roughening properties are customarily analyzed by measuring the *global* interface width:

$$W(L,t) = \langle \overline{[h(x,t) - \overline{h}]^2} \rangle^{1/2}, \tag{2}$$

where the overbar stands for spatial averages (in a system of size L) and brackets denote the disorder average. Usually, $W(L,t)$ obeys the Family–Vicsek dynamic scaling ansatz [1,2,15], namely

$$W(L,t) = t^{\alpha/z} f(L/\xi(t)), \tag{3}$$

where the scaling function $f(u)$ obeys

$$f(u) \sim \begin{cases} u^{\alpha} & \text{if} \quad u \ll 1 \\ \text{constant} & \text{if} \quad u \gg 1 \end{cases} \tag{4}$$

where α is the roughness exponent characterizing the stationary (or saturated) regime, $\xi(t) \sim t^{1/z}$ is the correlation length in the direction parallel to the interface, z the dynamic exponent and $\beta = \alpha/z$ is the growth exponent that governs the short-time behavior of the interface roughening. In particular, for 1D systems in the KPZ universality class $\alpha = 1/2$, $z = 3/2$ and $\beta = 1/3$ have been measured in an overwhelming variety of models and also experimentally [1–4, 6, 13].

Deviations from the previous values have also been reported in some experimental set-ups, for which it can be argued that the interfacial behavior is crucially affected by the presence of random pinning forces, i.e. by quenched disorder or heterogeneity in the physical background [1,2]. These situations can be addressed by replacing the noise term $\eta(\mathbf{x},t)$ in equation (1) with the quenched noised $\eta(\mathbf{x},h)$, accounting for spatial (quenched) heterogeneity:

$$\partial_t h(x,t) = \nu \nabla^2 h(x,t) + \lambda(\nabla h(x,t))^2 + F + \eta(\mathbf{x},h), \tag{5}$$

with $\langle \eta(\mathbf{x},h)\eta(\mathbf{x}',h') \rangle = \delta(\mathbf{x}-\mathbf{x}')\Delta(h-h')$ (where Δ is some fast-decaying function and F is an external driving force), which is known as the quenched Kardar–Parisi–Zhang (QKPZ) equation. This equation is usually complemented with the prescription that the interface is not allowed to move backwards (i.e. $\partial_t h(x,t) < 0 \to \partial_t h(x,t) = 0$). Equation (5) exhibits a pinning/depinning phase transition at a certain critical value of F_c, of the external driving force F [1,2], for $F > F_c$ the interfaces move with a finite velocity, while for $F < F_c$ they ineluctably become pinned by the impurities represented by the quenched noise.

Remarkably, the case in which the non-linearity moves in the same direction as the driving force ($\lambda > 0$) appears to differ qualitatively from the one in which these two forces oppose each other, ($\lambda < 0$) for the positive values of λ (i.e. the positive QKPZ or P-QKPZ equation) the depinning transition is smooth (second order), while for the negative ones λ (i.e. the negative QKPZ or N-QKPZ equation) it is abrupt (first order). The underlying reason for such a difference can be easily understood; taking equation (5) with quenched

J. Stat. Mech. (2014) P10024

noise, averaging over noise, integrating in x and imposing a stationary condition, one obtains

$$\lambda s^2 + F = 0 \tag{6}$$

where $s = \sqrt{\langle(\nabla h)^2\rangle}$ is the average local slope. This equation has a non-trivial solution with $s > 0$ if and only if $\lambda < 0$, corresponding to the pinned phase. This solution corresponds to the faceted interfaces of the average slope s and does not have a counterpart in the positive case $\lambda > 0$. Observe that the angle of the between facets θ, (see figure 1) obeys $s = \tan((\pi - \theta)/2) \propto 1/\sqrt{\lambda}$ and reaches a maximum value at the depinning transition.

The faceted solution ceases to exist at $F = F_c$, where the interface becomes depinned. Once the faceted solution breaks down, the interface velocity $\langle \partial_t h \rangle$ experiences a first-order transition and jumps from 0 to a constant stationary value. Even if the transition is discontinuous, the interface shows aspects of scale invariance both above and below the transition point. This type of hybrid situation sharing aspects of first order transition and scale invariance is known in the literature (see e.g. [16]).

Even if this simple argument suggests that the positive and negative cases should exhibit intrinsically different features, a renormalization group calculation reveals no difference between the positive and negative cases [17]. Indeed, the renormalized value of λ^2 diverges, suggesting the existence of a strong coupling fixed point for any value $\lambda \neq 0$. The renormalized value of λ^2 was measured in simulations of the N-QKPZ, revealing that it does not diverge, but stays finite even as the system approaches its critical point, suggesting that the renormalization group calculation might break down in this case. But the situation at this theoretical level has not been clarified thus far.

From the computational side, the QKPZ dynamics have been studied extensively for both positive and negative non-linearities in one spatial dimension. Tang *et al* [18] proposed that the P-QKPZ equation can be effectively described by the statistics of disorder pinning paths and, hence, mapped onto the so-called directed percolation depinning (DPD) model [19]. Thus, the roughness exponent is given by the ratio of the two correlation length exponents, in the parallel and perpendicular direction of the directed percolation cluster, namely $\alpha = \nu_\perp/\nu_{||}$ ($\simeq 0.63$); similarly it follows that $z = 1$ and hence $\beta = \alpha$. These results agree with the numerical simulations of systems in this class [20, 21]. On the other hand, numerical studies of different models with effective negative non-linearity confirmed the formation of facets and the existence of a jump at the transition [22–24].

Self-organized models, in which interfaces self-tune to the transition point [25], have also been proposed and studied in this context. Sneppen [26] proposed two different self-organized growth models in random media, one leading to facets and the other not and concluded that one lies in the N-QKPZ class, while the other behaves as a P-QKPZ. On the contrary, Choi *et al* [27] formulated two other similar self-organized models, with positive and negative non-linearities, respectively and concluded that the sign of the non-linear term does not affect the universality class.

Aiming at clarifying this very confusing state-of-affairs, here we revisit the P-QKPZ and N-QKPZ equations. Among other methods, we analyze the results by employing spectral techniques to establish whether the formation of facets and ultimately the sign of the non-linearity in the QKPZ equation, plays a relevant role or whether it does not.

J. Stat. Mech. (2014) P10024

2. Anomalous scaling

In some interfacial problems it is important to distinguish between global and local roughening properties. The *local* interface width $w(l,t)$ is defined as

$$w(l,t) = \langle \overline{[h(x,t) - \overline{h}]^2} \rangle^{1/2}, \tag{7}$$

where $\langle \cdots \rangle$ denote disorder average and the overbar an average over x in windows of l in size, obeying

$$w(l,t) = t^{\beta} f_A(l/\xi(t)), \tag{8}$$

where β is the growth exponent. Now the scaling function may be anomalous, i.e.

$$f_A(u) \sim \begin{cases} u^{\alpha_{\rm loc}} & \text{if} \quad u \ll 1 \\ \text{const} & \text{if} \quad u \gg 1, \end{cases} \tag{9}$$

where $\alpha_{\rm loc}$ is a new independent exponent called the local roughness exponent, which in general does not need to coincide with its global counterpart, α.

Ramasco *et al* introduced a general dynamic scaling ansatz for roughening interfaces, which includes all the previously-known forms of dynamic scaling as particular cases [24] (see also [28–30]). Implicit to this general scaling, ansatz is the hypothesis that the interface may exhibit two different types of behavior on short and long scales, respectively. The analysis relies on the structure factor or power spectrum $S(k,t)$):

$$S(k,t) = \left\langle \left| \frac{1}{\sqrt{L}} \int_0^L {\rm d}x h(x,t) {\rm e}^{-{\rm i}kx} \right|^2 \right\rangle, \tag{10}$$

where $k = 2\pi n/L$, with $n = 1, 2, ..., L-1$. The generic scaling ansatz for $S(k,t)$ proposed in [24] is

$$S(k,t) = k^{-(2\alpha+1)} s(kt^{1/z}), \tag{11}$$

with

$$s(u) \sim \begin{cases} u^{2\alpha+1} & \text{if} \quad u \ll 1 \\ u^{2(\alpha-\alpha_s)} & \text{if} \quad u \gg 1, \end{cases} \tag{12}$$

where α_s is the *spectral* roughness exponent. If $\alpha_s \neq \alpha$ there is anomalous scaling, while if $\alpha_s = \alpha$ the standard Family–Vicsek scaling is recovered. Remarkably, a new type of anomalous scaling behavior (with $\alpha = \alpha_{\rm loc} = 1$ and $\alpha_s > \alpha_{\rm loc}$) was theoretically predicted in [24] and one of the previously mentioned models by Sneppen (the one with facets) was argued to belong to this family.

Let us remark that—as emphasized by Ramasco *et al* [24]—α_s does not explicitly appear in the scaling behavior of either $W(L,t)$, $w(l,t)$ or the height–height correlation function $G(l,t)$ and, thus, cannot be deduced from the measurements of these quantities, suggesting that a sound study of the roughening properties should include spectral analyses.

doi:10.1088/1742-5468/2014/10/P10024

J. Stat. Mech. (2014) P10024

3. Results

We solved equation (5) numerically with both positive and negative non-linearities in one dimensional lattices and studied its spectral properties. Therefore, we consider a standard finite-differences discretization scheme for equation (5) in rings the size of L (i.e. periodic boundary conditions are assumed) [2, 20, 23]. More refined algorithms such as the one proposed in [31] could be implemented, but they are not necessary for our purposes here. Time is discretized in units of $\Delta t = 0.01$, $\nu = 1$ and, following previous analyses [23], the noise is taken to be uniformly distributed in $[-a/2, a/2]$ with $a = 4.642$. Initial conditions correspond to a flat interface of $h(x, t = 0) =$ constant. A fresh value of the quenched random force is extracted at position x whenever the interface advances to such a point; this value is kept fixed until the interface moves forward again. Ensemble averages are performed over at least 1000 different realizations of the quenched randomness. The results have been verified to be robust against changes in these choices.

3.1. $\lambda > 0$ (P-QKPZ)

Figure 1(a) shows interface profiles for the P-QKPZ case (with $\lambda = 0.5 > 0$ and $F = 1$): the interface grows until it becomes eventually pinned for $F < F_c$. The measured roughness exponent at the transition point is $\alpha = 0.63(1)$ in good agreement with the expectation for the DPD class. Given that the universality of this class is well understood [1, 2], we have not performed further extensive numerical studies of this positive λ case.

3.2. $\lambda < 0$ (N-QKPZ)

Figure 1(b) shows a profile in the N-QKPZ case ($\lambda = -0.5 < 0$) obtained close to the transition point $F_c \approx 1.98$. Observe the distinct shape of the pinned interfaces exhibiting, as expected, characteristic facets. In agreement with previous findings, we observe a first-order pinning–depinning transition, at which the averaged interfacial velocity jumps discontinuously from zero to a positive constant value.

3.2.1. The depinned phase. For sufficiently large driving forces—deep into the depinned or moving phase—the quenched disorder should be irrelevant above some length and time scales and the freely moving interface should therefore follow standard KPZ dynamics. Indeed, taking $F = 3 \gg F_c$ (see figure 2) we find that $S(k, t)$ scales in the large-time regime scales as a power law with the exponent $2\alpha + 1 = 2.03(4)$, i.e. with $\alpha = 0.515(20)$, as corresponds to standard non-anomalous Family–Vicsek behavior (see the collapse obtained in the inset of figure 2 with $\alpha = 1/2$ and $z = 3/2$). Therefore, the moving interface belongs to the standard KPZ universality class, as expected.

3.2.2. The pinned phase. More interesting is the behavior of $S(k)$ for stationary pinned interfaces $F < F_c$. Figure 1(b) shows the results for a single realization; it illustrates the development of a (single) well-defined pinning center close to $x = 100$, at which the interface eventually becomes fully pinned. A careful inspection of figure 1(b) reveals that the slopes around the peak are not just straight lines but they have some intrinsic roughness. Therefore, two different regimes are expected to emerge when computing the structure function,

J. Stat. Mech. (2014) P10024

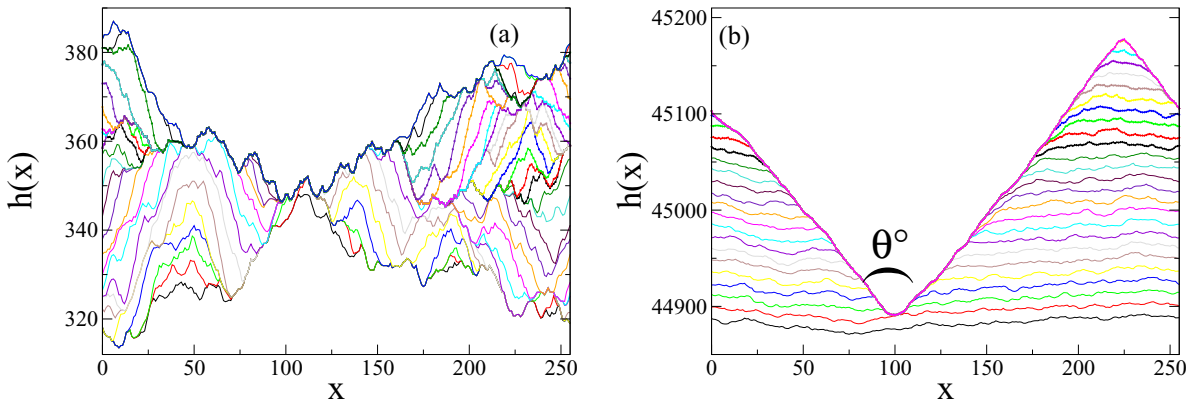

Figure 1. Time evolution of a KPZ interface moving in a $(1+1)-$dimensional disordered medium (system size $L = 256$). (a) **P-QKPZ** case with $\lambda = 0.5$, $F = 1.00 < F_c$) and different times (from bottom to top $t = 199\,000$ to $t = 232\,000$ at uniform intervals). (b) **N-QKPZ** case with $\lambda = -0.5$ and $F = 1.90 < F_c$) for different times (from bottom to top $t = 4\,030\,000$ to $t = 4\,055\,000$ at uniform intervals). The average angle at the bottom of the valley, $\theta = 49(2)^\circ$, was obtained by averaging over 100 different pinned interfaces.

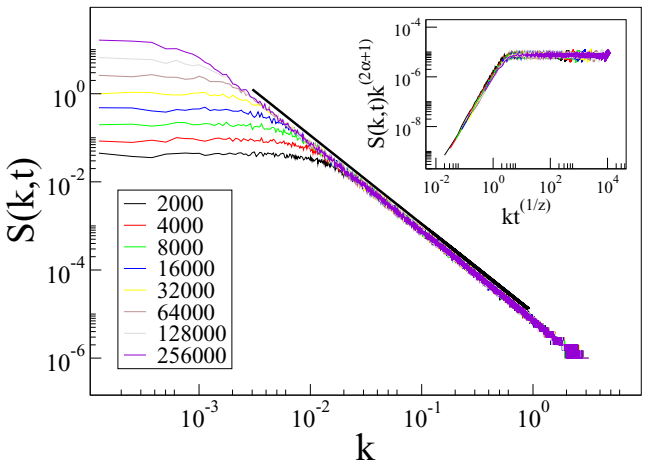

Figure 2. Supercritical behavior in the N-QKPZ case: double logarithmic plots of the structure factor $S(k)$ versus the wave number k obtained for different times for $F = 3 \gg F_c$, $L = 50\,000$ and averaging over 250 configurations. The continuous straight line is a fit of the long-k regime and has been slightly shifted upwards for the sake of clarity. It has a slope of $-2.03(4)$ yielding $\alpha = 0.51(2)$. The inset shows a data collapse obtained using the equation (12) with $\alpha = 1/2$ and $z = 3/2$.

corresponding to linear slopes and fluctuations on top of them, respectively. This suggests the existence of anomalous scaling. Indeed, as shown in figure 3, $S(k)$ exhibits a crossover between short and large k regimes at a certain crossover value of k_c. Observe that, as illustrated in the inset of figure 3, the crossover between short and long scales is rather insensitive to changes in F and L, revealing the absence of a diverging correlation length.

J. Stat. Mech. (2014) P10024

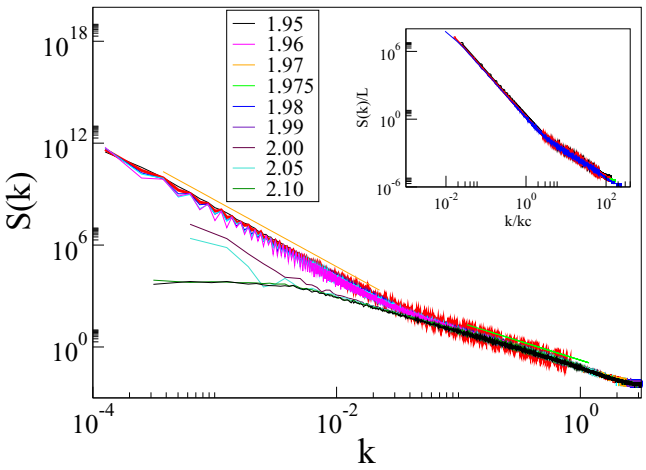

Figure 3. Double logarithmic plot of the structure function, $S(k)$ for the N-QKPZ case for both subcritical and supercritical values of F (system size $L = 5000$). The continuous straight lines are the fits of the large-k regime (slope $-2.1(2)$, i.e. $\alpha = 0.55(5)$) and the small-k regime for subcritical forces (slope $-3.99(2)$, i.e. $\alpha_s = 1.49(2)$), respectively. The fits have been slightly shifted upwards for visual clarity. Some supercritical values of F have been included in the plot to illustrate that the short-scale behavior is indistinguishable in both cases and is compatible with $\alpha = 1/2$. Inset: log–log plots of the structure factor in the subcritical regime, rescaled to system size, versus $k/k_c(L)$, where $k_c(L)$ is the value of k at which the crossover occurs, obtained for samples of different side L, i.e. $L = 10\,000, L = 20\,000, L = 50\,000, L = 100\,000, L = 200\,000$ and for $F = 1.95 < F_c$. A nice curve collapse is observed.

The structure function of the pinned interfaces (see figure 3) clearly shows two well-separated regimes; the small-k (large wavelength) limit describes the facets, while the large-k (short wavelengths) corresponds to the fluctuations existing on the top of the two facets. From the slopes of the curve, as shown in figure 3, we obtain $\alpha_s = 1.49(2)$ in the small-k regime, i.e. for the macroscopic faceted structures. Let us remark, that for the trivial case of a perfectly faceted interface formed by identical segments, it is not difficult to show that the spectral roughness exponent is $\alpha_s = 3/2$ [24]. On the other hand, we measure $\alpha = 0.55(5)$ for the large-k (small wavelength) regime, which corresponds to the roughness that 'modulates' the slopes of the facets. This value is compatible with $\alpha = 1/2$, as obtained for depinned interfaces.

3.3. Global and local roughening

Now we present the results obtained using the standard measurements of the global and local interface roughness, (equations (2) and (7), respectively). Figure 4 shows the log–log plots of the global interface width versus time, obtained for $F = 1.90 < F_c$. Two types of average are presented, either the overall runs (labelled *all*), or restricting the average to the moving interfaces (label *moving*). Observe that the averages including all the runs (and thus, the pinned faceted interfaces) have a greater degree of roughness.

J. Stat. Mech. (2014) P10024

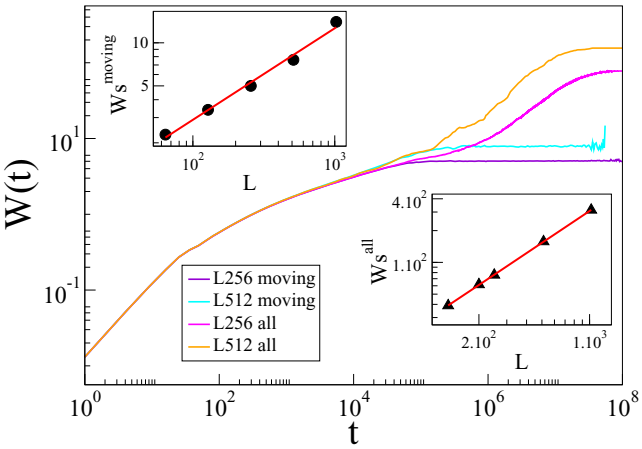

Figure 4. Global interfacial width in the N-QKPZ case. (a) Log–log plots of the global width W versus t, obtained for $F = 1.90 < F_c$ and samples of different sizes, averaged over *all* realizations or restricted to *moving* interfaces (two curves, corresponding to 2 different sizes are represented). Upper inset: log–log plot of the (stationary) saturation value of the global width W versus sample size L, for moving interfaces obtained for 5 different system sizes (including the 2 sizes in the main plot). The best fit of the straight line yield $\alpha^{\text{moving}} \approx 0.53$. Lower inset: as the upper inset, but averaging over all the runs (pinned and moving; the best fit gives $\alpha^{\text{all}} = 1.003(8)$).

The roughness exponents corresponding to the global width measured for the depinned interfaces $\alpha^{\text{moving}} \approx 0.53$, is consistent with the value obtained for the large-k regime of the structure factor. Thus, the global width of the moving interfaces captures the roughness that 'modulates' the slopes of the facets. On the other hand, once pinned (i.e. faceted) and the interfaces are taken into account, we obtain $\alpha^{\text{all}} \approx 1$, implying that the scaling is dominated by the linear facets.

Figure 5 shows log–log plots of the local width $w(l, t)$ (see equation (8)), versus l obtained for different times. The measurements done for the pinned interfaces (in the $t \to \infty$ limit) allow us to determine $\alpha_{\text{local}} = 0.997(5)$, confirming that for the pinned interfaces, both the local and the global roughness exponents are asymptotically controlled by the faceted structure. On the other hand, employing the scaling form $w(l, t) \sim l^{\alpha} F(l/\xi)$, where F is a scaling function and ξ is a saturation or correlation length (i.e. the value of l above which a constant local width is measured) and using $\alpha = 1$, we obtain a good collapse, as illustrated in the right of figure 5 (see also similar scaling laws for the pinned and depinned phases, in [32]).

3.4. Direct analysis of local fluctuations modulating facets

Figure 6(a) shows a snapshot of a pinned configuration; the slopes of the faceted structure have been adjusted by two straight lines. On top of these linear structures there are fluctuations, as illustrated in the inset of figure 6(a), where the average slope has been locally subtracted. By computing the variance (R) around the linear fits for facets of different linear sizes, we obtain the local width as a function of the facet linear size, l (see

J. Stat. Mech. (2014) P10024

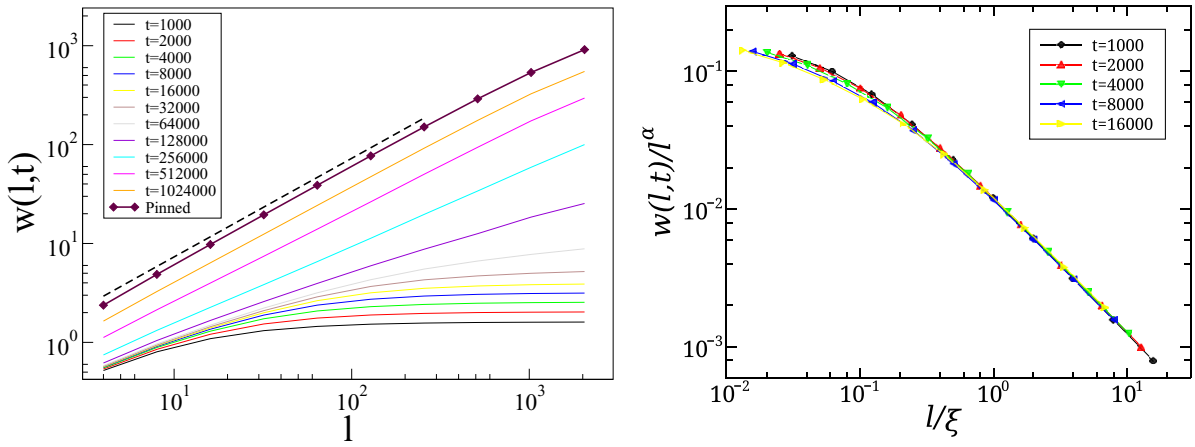

Figure 5. Left: local interfacial width in the N-QKPZ case. Log–log plots of the local width of the interface $w(l,t)$ versus l obtained for the samples measuring $L = 4096$ and different measurement times, as indicated, in the pinned phase ($F = 1.90 < F_c$ and averages over 500 configurations). Initially the interfaces are flat and then, progressively, roughness develops. Diamonds indicate pinned interfaces and the dash (which has been moved for the sake of clarity) shows the best fit, corresponding to $\alpha_{\rm loc} = 0.997(5)$. Observe that the range in which the linear scaling can be observed grows as time increases and the facets develop. Right: the curve collapse is obtained using the scaling form $w(l,t) \sim l^{\alpha} F(l/\xi)$ for times up to $t = 16\,000$; for longer times a saturation length of ξ cannot be properly measured.

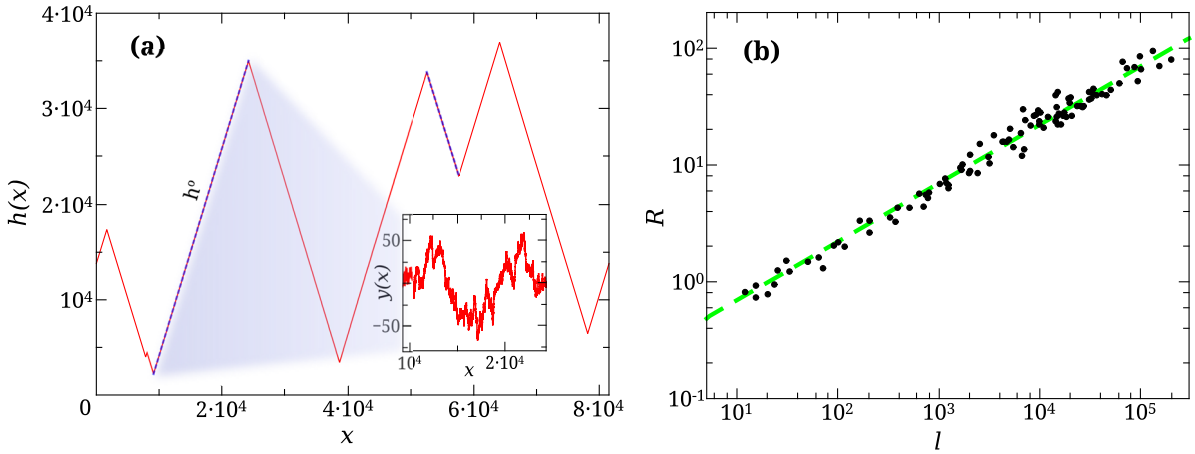

Figure 6. Analysis of local scale fluctuations in the N-QKPZ. (a) An example of a pinned interface with $\lambda = -0.5$ and $F = 1.94$. The slopes of the facets can be linearly fitted (straight dashes with a slope h°), allowing us to estimate the slope and the mean squared error R around it. Inset: Zoom of the local fluctuations $y(x)$ around one of the facets. (b) Log–log plot of R ($w_{\rm local}$) versus the linear size of the facets (the lines are guides for the naked eye). The best fit is obtained for a local roughness exponent of 0.51(1), close to the KPZ value of $\alpha = 1/2$.

J. Stat. Mech. (2014) P10024

figure 6(*b*)). It follows that the data can be very well-fitted into a double-logarithmic plot by a straight line with a slope of 0.51(1), again suggesting a local roughness compatible with $\alpha = 1/2$.

4. Discussion and conclusions

We have presented a full characterization of the interfacial growing behavior of the KPZ equation with quenched noise and a negative value of the coefficient in the non-linear term (see equation (5)). The positive case exhibits a continuous phase transition in the DPD universality class, while in the negative case we have found evidence of a discontinuous transition separating a pinned phase, characterized by faceted interfaces and a moving KPZ-like phase. Our study is focused on the negative case and our main conclusions are:

(a) The measurements of the structure factor of the pinned interfaces show anomalous scaling behavior, which can be considered as a particular case of the general scaling theory proposed by Ramasco *et al* as applied to the pinned interfaces (i.e. with no explicit time dependence). $S(k)$ exhibits a crossover between the small-k regime with $\alpha_s \approx 1.5$ (controlled by facets) and the large-k regime with $\alpha \approx 0.55$.
(b) The standard measurements of the local and global widths and the analysis of its scaling behavior within the pinned phase ($F < F_c$) yield $\alpha_{\rm local} \approx \alpha^{\rm all} \approx 1$. However, by excluding the pinned (faceted) interfaces in the calculation of the average we obtained $\alpha^{\rm moving} \approx 0.53$, consistent with the large-k scaling of the structure factor.
(c) Finally, the direct measurements of the fluctuation around the facets reveal that local fluctuations can be well-represented by the roughening exponent $\alpha \approx 0.51$.

All these results put together suggest that local roughening is controlled by the standard KPZ roughening exponent. This result is in agreement with the finding in [33] for a similar interfacial model with columnar disorder (i.e. $\eta = \eta(x)$); this model was reported to exhibit facets with roughness profiles on top of them, controlled by a 0.5 exponent. Furthermore, in this same work [33], the authors showed analytically that the dynamics of facets can be decoupled from short-scale fluctuations and that these latter ones exhibit KPZ roughness. An almost identical calculation leads us to the same conclusion here: local and global dynamics are decoupled; on the one hand there are facets and on the other there are short-scale KPZ-like fluctuations.

Therefore, we have not found any evidence of continuous transitions, nor of roughness exponents around 0.63, characteristic of the DPD class in the negative case and we can safely conclude that the two cases, with both positive and negative non-linearities, are clearly different. Obviously, the origin in this difference stems from the facet formation in the negative case; thus it would be reasonable to conjecture that by running simulations in tilted systems—with a tilt equal or larger to the critical slope—there should not be an abrupt transition between the faceted and non-faceted/moving interfaces. One should not observe a continuous transition and exponent values at the transition point compatible with DPD class, as indeed numerically verified in [22].

Further to this new study, some important questions remain unsolved and the study of interfaces in random media remains an intriguing research area. For example, analyzing

J. Stat. Mech. (2014) P10024

in detail what happens in physically, more relevant and higher dimensional systems (e.g. in two dimensions), where pinning paths (and thus DPD) are expected to be replaced by 'pinning surfaces' [34], is left for future investigation.

Interestingly, a similar physical situation arises in the study of KPZ interfaces bounded by a wall, which is relevant in the study of non-equilibrium wetting [35, 36] and synchronization transitions [37]. Under these circumstances, the case $\lambda > 0$ has been shown to be radically different from the $\lambda < 0$ one; the corresponding associated problems have very different physical behavior and they belong to two distinct universality classes [38]. Therefore, it seems that under diverse circumstances, positive and negative KPZ non-linearities describe very different situations.

Acknowledgments

We acknowledge financial support from Acción Integrada hispano-argentina, AR2009-0003; MAM acknowledges support from J de Andalucía project of Excellence P09-FQM-4682 and from the Spanish MEC project FIS2009-08451. BM and EVA acknowledge the financial support of CONICET (PIP-0143) and UNLP (Argentina). We are thankful to F de los Santos, J A Bonachela and J M López for useful discussions and/or critical reading of the manuscript.

References

[1] Halpin-Healy T and Zhang Y C 1995 *Phys. Rep.* **254** 215–414
[2] Barabási A L and Stanley H 1995 *Fractal Concepts in Surface Growth* (Cambridge: Cambridge University Press)
[3] Krug J and Spohn H 1990 *Solids Far from Equilibrium* (Cambridge: Cambridge University Press)
[4] Krug J 1997 *Adv. Phys.* **46** 139–282
[5] Kardar M, Parisi G and Zhang Y C 1986 *Phys. Rev. Lett.* **56** 889
[6] Takeuchi K and Sano M 2010 *Phys. Rev. Lett.* **104** 230601
[7] Takeuchi K, Sano M, Sasamoto T and Spohn H 2011 *Sci. Rep.* **1** 34
[8] Johansson K 2000 *Commun. Math. Phys.* **209** 437–76
[9] Sasamoto T and Spohn H 2010 *Phys. Rev. Lett.* **104** 230602
[10] Calabrese P and Le Doussal P 2011 *Phys. Rev. Lett.* **106** 250603
[11] Prähofer M and Spohn H 2000 *Phys. Rev. Lett.* **84** 4882
[12] Canet L, Chaté H, Delamotte B and Wschebor N 2010 *Phys. Rev. Lett.* **104** 150601
[13] Huergo M, Pasquale M, Bolzán A, Arvia A and González P 2010 *Phys. Rev.* E **82** 031903
[14] Moglia B, Guisoni N and Albano E 2013 *Phys. Rev.* E **87** 032713
[15] Family F and Vicsek T 1985 *J. Phys. A: Math. Theor.* **18** L75
[16] Liggett T 2004 *Particle Systems* (Berlin: Springer)
[17] Stepanow S 1995 *J. Physique (France)* II **5** 11–7
[18] Tang L H and Leschhorn H 1993 *Phys. Rev. Lett.* **70** 3832–2
[19] Buldyrev S, Barabási A L, Caserta F, Havlin S, Stanley H and Vicsek T 1992 *Phys. Rev.* A **45** R8313
[20] Leschhorn H 1996 *Phys. Rev.* E **54** 1313–20
[21] Lee C and Kim J 2005 *J. Korean Phys. Soc.* **47** 13–7
[22] Jeong H, Kahng B and Kim D 1996 *Phys. Rev. Lett.* **77** 5094–7
[23] Jeong H, Kahng B and Kim D 1999 *Phys. Rev.* E **59** 1570–3
[24] Ramasco J J, López J and Rodríguez M 2000 *Phys. Rev. Lett.* **84** 2199
[25] Dickman R, Muñoz M, Vespignani A and Zapperi S 2000 *Braz. J. Phys.* **30** 27–41
[26] Sneppen K 1992 *Phys. Rev. Lett.* **69** 3539

J. Stat. Mech. (2014) P10024

[27] Choi Y M, Kim H J and Kim I M 2002 *Phys. Rev.* E **66** 047102
[28] Ramasco J, López J and Rodríguez M 2001 *Phys. Rev.* E **64** 066109
[29] López J, Rodríguez M and Cuerno R 1997 *Phys. Rev.* E **56** 3993
[30] López J, Rodríguez M and Cuerno R 1997 *Physica* A **246** 329–47
[31] Lam C H and Shin F 1998 *Phys. Rev.* E **58** 5592–5
[32] Makse H A and Nunes Amaral L A 1995 *Europhys. Lett.* **31** 379
[33] Szendro I, López J and Rodríguez M 2007 *Phys. Rev.* E **76** 011603
[34] Barabási A L, Grinstein G and Muñoz MA 1996 *Phys. Rev. Lett.* **76** 1481
[35] de Los Santos F, Da Gama M T and Muñoz M A 2002 *Europhys. Lett.* **57** 803
[36] de Los Santos F, Da Gama M T and Muñoz M A 2003 *Phys. Rev.* E **67** 021607
[37] Muñoz M A and Pastor-Satorras R 2003 *Phys. Rev. Lett.* **90** 204101
[38] Muñoz M A, Korutcheva E and Cuerno R 2004 *Advances in Condensed Matter and Statistical Mechanics* (New York: Nova Science)

J. Stat. Mech. (2014) P10024